This is the author's final accepted version.

There may be differences between this version and the published version. You are advised to consult the publisher's version if you wish to cite from it.

http://eprints.gla.ac.uk/154632/

Deposited on: 03 January 2018

An integrated kinetic model for downdraft gasifier based on a novel approach that optimises the reduction zone of gasifier

AHMED M. SALEM[1,2] and MANOSH C. PAUL[1*]

[1]Systems, Power & Energy Research Division, School of Engineering, University of Glasgow, Glasgow, G12 8QQ, UK

[2]Mechanical Power department, Faculty of Engineering, Tanta University, Egypt

Email: a.salem.2@research.gla.ac.uk, *Manosh.Paul@glasgow.ac.uk

Tel: +44 (0)141 330 8466

Abstract

A kinetic model was built to estimate the optimum working parameters of a downdraft gasifier, in which a set of chemical kinetics at each zone of the gasifier was described. The model deals with a wide range of biomass types with elemental composition ranges of (38≤C≤52) %, (5.5≤H≤7) %, and (36≤O≤45) %. This model is able to predict gas composition, tar content, temperature and height of each zone, as well as temperature, velocity and pressure distribution at reduction zone with heating value of product gas. The model also gives full design dimensions of a downdraft gasifier. The final results, which proved to be in a good agreement with experimental works under different working conditions of biomass type, moisture content, and air-to-fuel ratio, are based on a new approach that includes calculation of the optimum height of the reduction zone. Calculation based on the optimum height ensures that all the char produced is consumed in the reduction zone, thus leading to the production of the maximum amount of gases. Results conclude that biomass with a moisture content less than 10% and equivalence ratio of 0.3-0.35 leads to the production of higher yield of syngas with low tar content. In particular, woody biomass materials are found to give the higher heating value for producer gas with a reasonable amount of tar.

Keywords: Downdraft gasifier, Kinetic model, Producer gas, Gasification, Biomass.

1.   INTRODUCTION

The world is continuously looking for new alternative sources for energy production which are clean, sustainable and renewable. Biomass, which is considered to be one of the most promising alternatives for fossil fuels nowadays, can be converted into solid, liquid and gaseous fuels for generating energy. Additionally, biomass does not contribute to the greenhouse effects, which is therefore an advantage against the fossil fuels. Besides it is a renewable source of energy. Therefore, researchers are working for the energy production using biomass ([1], [2], [3], [4], [5], and [6]).

The most common use of biomass for energy is direct combustion, followed by gasification, carbonization, and pyrolysis [1]. Biomass gasification is one of the most promising techniques to convert solid fuels into useful gaseous fuels which can be broadly used in many industrial applications such as in combined heat and power generation [6] and internal combustion engines for various means of transportations. Gasification is a thermochemical process that converts a solid fuel into a gaseous fuel at temperatures around 900°C. It produces CO, H_2 and small amounts of CH_4 as desired products with other undesired gases like N_2, CO_2, and other hydrocarbons (HC).

Modelling biomass gasification is a favourable technique that can simulate the gasifier design, output parameters, working conditions, etc. It is understood that a pure thermodynamic model cannot predict the product gas of a gasifier because it gives an over prediction for the higher heating value (HHV) and the H_2 output. And a thermodynamic model also predicts the lower amounts of CO but with the higher amounts of CH_4 [5]. Altafini et al. [7] presented a kinetic model taking into account that the reduction reactions are generally slower than the oxidation reactions by several orders of magnitude. The way to measure these effects is driven through the reaction rates which are the key for identifying the reaction formations and rates. Using high temperatures for the reduction reactions, the equilibrium model products may deviate from their reality due to the kinetic constant variations which strongly affect the gas composition. Thus, the kinetic models are more suitable and accurate to predict the gas composition.

However, the previous kinetic and equilibrium models have some limitations. Budhathoki [8] introduced a model based on the combination between the kinetic approach for the reduction zone and the thermodynamic equilibrium for the other zones. This model was compared with other experimental works for wood biomass and was found to be in a good agreement for gas

composition except for methane in which it gave higher prediction rates. Ratnadhariya and Channiwala [9] proposed a new model for modelling biomass gasification. It is composed of three different zones, in which drying and pyrolysis is the first zone followed by the combustion and reduction zones. The model is a combined system of the stoichiometric model with assumptions for the pyrolysis and oxidation zones for predicting the output gases. This model provides the operating range for the woody biomass materials only. While Dejtrakulwong et al. [10] built a four-zone kinetic model showing the effect of moisture content and air-to-fuel ratio on the temperature and height of each zone, which is useful in gasifier design evaluation.

Additionally, the kinetic models presented in the published literatures have further limitation and lack depth in reporting some details like biomass variety, tar formation and optimum working conditions. For instance, Budhathoki [8] reported that his model is only valid for wood biomass material, and it does not take into account any tar formation and higher hydrocarbons. Several other researchers (e.g. see [11], [12]and [13]) only discussed the effect of changing biomass moisture content on the producer gas composition and its heating value, and they showed that a higher moisture content reduces the heating value. However, they did not show any possible effects on the residuals and tar content. Furthermore, they did not discuss the effect of other working parameters like the equivalence ratio. A thermochemical equilibrium model developed by [14] predicts biomass gasification of different biomass materials with effect of moisture content and air-to-fuel ratio on the producer gas heating value, but again this study excludes tar content and discussion on the producer gas quality. We develop a four-zone integrated kinetic model allowing to investigate the effect of moisture content and air-to-fuel ratio on the temperature and height of each zone, which is useful in gasifier design evaluation. The current kinetic model will focus on these challenges and try to address the issues highlighted above.

Moreover, all the previously published articles discussed the gasification kinetic model with a constant height of the reduction zone of gasifier (e.g. see [9] , [10], [15], and [16]). Based on the review, this is the first time the model presented in this work incorporates the effect of height of the reduction zone on the concentration of different species of product gases as predicted. Taking into account a wide range of biomass materials covered by the model, the study will also focus on the prediction of tar content and try to find the optimum working conditions leading to the production of high quality syngas as well as biomass materials that

give a higher yield of syngas with a low tar content. The model will further provide useful information for the full design of a downdraft gasifier based only on a desired thermal power. Further to be noted that to the best of our knowledge, there appears to be no previous model that includes the product gas composition, tar content and a full design of gasifier. The model will address the gasifier design based on the key parameters like the throat diameter and fuel feeding rate and its effect on other working parameters.

2.   MODELING PROCEDURE

The proposed model is built through a set of chemical kinetic schemes to predict the full design principles for a downdraft gasifier which depends on a series of reactions taking place in the gasifier. Biomass gasification is done through the four main steps: drying, pyrolysis, oxidation and gasification / reduction as shown in Figure 1. A schematic drawing of a downdraft gasifier is shown in which biomass is fed from the top of the gasifier into the drying zone and air is fed into the oxidation zone for combustion process and then the product gas is driven from the down of the gasifier. The tar is collected in the bottom.

The model is assumed to be 1D, and all char is consumed in the reduction zone and air is used as a gasifying medium. Modelling involves an integration of the four zones and the thermochemical kinetic processes associated with the main zone elaborately explained in the following sections. The output of each zone of gas composition is considered as an input for the next one based on Figure 1.

2.1   Drying Model

The drying zone receives heat from oxidation which leads to an increase of temperature. The initial temperature is supposed to be 298 K, however when the temperature reaches 368 K, the vaporization of moisture content starts until it reaches 473 K as mentioned by [10]. At this temperature the pyrolysis begins automatically, thus the devolatization of biomass occurs [10]. The rate at which the drying reaction taking place is determined by the equation below ([10] and [17]). Constant drying temperature is used in calculations as 400 K to ensure that the drying process is complete.

$$r_d = K_d . C_{H_2O,l},\tag{1}$$

$$K_d = A_d \exp\left(\frac{-E_d}{R\,T_d}\right),\tag{2}$$

Where, the constants used in the drying model are summarised in Table 1.

2.2 Pyrolysis Model

Biomass after drying first decomposes into volatiles and char, then these components further react with each other to form char and volatiles again as shown in Figure 2. Volatiles contain gases such as CO, CO_2, CH_4, H_2 and H_2O, as well as other hydrocarbons, tar and sulphur components. The release of volatiles however depends on the ultimate analysis of a biomass and its volatile and ash content. The chemical reaction processes occurring in the pyrolysis zone are described by the kinetic equations in Eqns. (3-9), [18].

$$\frac{dC_B}{dt} = -K_1 C_B^{n1} - K_2 C_B^{n1}, \tag{3}$$

$$\frac{dC_{G1}}{dt} = K_1 C_B^{n1} - K_3 C_{G1}^{n2} C_{C1}^{n3}, \tag{4}$$

$$\frac{dC_{C1}}{dt} = K_2 C_B^{n1} - K_3 C_{G1}^{n2} C_{C1}^{n3}, \tag{5}$$

$$\frac{dC_{G2}}{dt} = K_3 C_{G1}^{n2} C_{C1}^{n3} = \frac{dC_{C2}}{dt}, \tag{6}$$

Where,

$$K_1 = A_1 \, exp[\,(D_1/T) + (L_1/T^2)], \tag{7}$$

$$K_2 = A_2 \, exp[\,(D_2/T) + (L_2/T^2)], \tag{8}$$

$$K_3 = A_3 \, exp[\,(-E/RT)]. \tag{9}$$

Equation (3) shows the decomposition of virgin biomass C_B with time, while equations (4(6) represent the decomposition of gases and char respectively to form the final concentration of char and volatiles (gases) into two steps. The kinetic constants used for these equations are illustrated in equations (7(9) where *A*, *D*, and *L* are the best fit values of the kinetic parameters of the primary pyrolysis reactions and their values are illustrated in Table 2. The following initial conditions are used for solving the coupled ordinary differential equations (3)-(9), e.g. at $t = 0$, $C_B = 1$ and $C_{G1} = C_{C1} = C_{G2} = C_{C2} = 0$.

Babu et al. [18] determined the optimum parameters for pyrolysis through a wide range of heating values and temperatures during isothermal and non-isothermal processes and found that the optimum conditions for non-isothermal process are as stated in Table 3. Optimum parameters ensure that all biomass successfully converted into volatiles and char and final concentration of virgin biomass left is less than 0.03. While they showed that the optimum temperature for pyrolysis is 1259 K, the temperature is still very high to handle before

oxidation and this will require a higher temperature in the oxidation zone plus specific design materials for gasifier. As a consequence we choose a temperature of 873 K as an initial guess for the solution, as the pyrolysis process is very slow below 773K as reported by [10]. This is then followed by solving the pyrolysis and energy balance equations to determine the actual temperature and using this, the pyrolysis products are finally calculated. The volatiles are assumed to be CO, CO_2, CH_4, H_2, H_2O, and tar. The importance of this part is that it gives the final concentration of char and volatiles; after which the concentration of char is known at the end of devolatization and is used for the next step in which the volatiles concentration is predicted.

Sharma [16] introduced a new model to predict the percentage composition of volatiles and he considered a one-step model for the biomass pyrolysis as follows

$$C_a H_b O_d \rightarrow x_1 C + x_2 CO + x_3 CO_2 + x_4 CH_4 + x_5 H_2 + x_6 H_2O + \quad (10)$$
$$x_7 C_6 H_{6.2} O_{0.2},$$
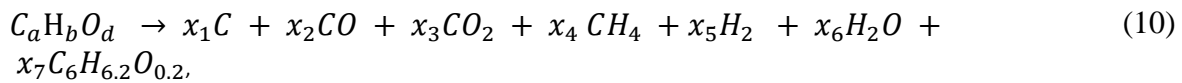
Where $C_a H_b O_d$ represents biomass, x is the concentration of different species of pyrolysis products in mol, $C_6 H_{6.2} O_{0.2}$ is the tar chemical formula as considered by many researchers e.g. [16]. The mass fraction (Y/Y) empirical relations used are;

$$\frac{Y_{CO}}{Y_{CO_2}} = exp(-1.845 + \frac{7730.3}{T} - \frac{5019898}{T^2}), \quad (11)$$

$$\frac{Y_{H_2O}}{Y_{CO_2}} = 1, \quad (12)$$

$$\frac{Y_{CH_4}}{Y_{CO_2}} = 5 \times 10^{-16} \times T^{5.06}. \quad (13)$$

2.3   Oxidation Model

The oxidation zone supplies the required heat for drying and pyrolysis. Biomass combustion requires gasifying medium (air) to complete. If the air is less than the stoichiometric amount required, the gasification (reduction) process will take place to produce syngas. The oxidation process taking place through the chemical reactions are illustrated in Table 4 and

Table 5. Pyrolysis products are oxidized in an order that depends on the reaction rate [16] as follows;

- Oxidation of all the hydrogen completes first (R1).
- Oxidation of CO then takes place (R2).

- If oxygen still remains, it will oxidize methane from pyrolysis (R3).

- And if more oxygen is available, it will oxidize tar and char according to their reaction rates (R4 and R5).

An energy balance is made for the combustion stage to determine the oxidation temperature based on equation (14)

$$\sum X_i \cdot \left(h_f + C_p \cdot \Delta T \right)_{\text{pyrolysis products}} = \sum X_i \cdot \left(h_f + C_p \cdot \Delta T \right)_{\text{combustion products}} + \quad (14)$$
$$Q_{\text{loss}}$$

The heat loss is mentioned in the oxidation zone only as it is higher in temperature than other zones, and the overall heat loss is assumed to be 10% of the product of the equivalence ratio (ER) and HHV [19] . The same energy balance principle is made for the pyrolysis and reduction zones.

Based on the energy balance, assumptions only were made for the inlet temperature (298 K), then the temperature profile along the gasifier was calculated.

2.4   Reduction model

Production of producer gases starts from the reduction zone and hence, a detailed kinetic model was also used at this zone to determine all the data required along the reduction zone length/height. The change in mole fractions of any gas species at the reduction zone along the distance *z* (reduction height/length) is determined by [10] ;

$$\frac{dn_x}{dz} = \frac{1}{v}\left(R_x - n_x \frac{dv}{dz} \right) \qquad (15)$$

The reactions considered for the reduction zone are illustrated in Table 6. Reaction rates r_i are given in Table 7 .

Velocity, temperature, and pressure variations along the reduction zone are obtained through the solution of the following differential equations *[15]*

$$\frac{dv}{dz} = \frac{1}{\sum_i n_i C_{pi}} \left[\frac{\sum_i n_i C_{pi} \sum_i R_i}{n} - \frac{\sum_i r_i \Delta H_i}{T} - \frac{dP}{dz}\left(\frac{v}{T} + \frac{v \sum_i n_i C_{pi}}{P} \right) - \sum_i R_i C_{pi} \right] \quad (16)$$

$$\frac{dT}{dz} = \frac{1}{v \sum_i n_i C_{pi}} \left[\sum_i r_i \Delta H_i - v\frac{dP}{dz} - p\frac{dv}{dz} - \sum_i R_i C_{pi} T \right] \qquad (17)$$

$$\frac{dP}{dz} = 1183\left(\frac{\rho_{gas}}{\rho_{air}} v^2 \right) + 388.19\, v - 79.896 \qquad (18)$$

In the numerical solution procedure, the set of governing equations stated above is discretized by dividing the reduction zone into equal small zones and solved simultaneously. The initial conditions or the inlet conditions of the reduction zone are taken from the outputs of the combustion zone. The initial pressure and temperature at the reduction zone inlet were assumed to be 1.005 atm, and 1300 K based on ([20], [16]). The equations were solved with a Matlab code *ode45* which is based on an explicit Runge-Kutta 4th order accurate scheme, giving the residual tolerances in the order of 10^{-6}. Concentration of the product gases, velocity, temperature, and pressure distribution in the reduction zone are obtained and discussed in the result sections.

2.5 Gasifier design principles

The velocity of pyrolysis gas flow through the gasifier is calculated from the following equations [10];

$$v_g = \frac{2RT_p}{P} \sum_{i}^{n} N_{g,i} \tag{19}$$

$$N_{gi} = \frac{4 \, x_{gi} \, m_b}{\pi \, D^2} \tag{20}$$

The biomass feeding rate is calculated from Rathore [21] based on the input thermal power (W_{th}) of a gasifier

$$\dot{m}_f = \frac{W_{Th}}{HHV_f} \tag{21}$$

Equation (22) describes how the throat diameter at the end of combustion zone is calculated.

$$GH = \frac{2.5 \, \dot{m}_f}{A_{th}} \tag{22}$$

The hearth load (*GH*) is defined as the amount of produced gas at normal conditions per unit area of throat [21]. The recommended value of *GH* is within the range of 0.1-1 [22] and [21], so a value of 0.35 is used in our calculations based on [22] and [23]. In addition, [24] reported that the throat angle of around 45° gives a higher conversion efficiency though in some studies a throat angle of 60° is also recommended. After calculating the throat diameter, the fire box (pyrolysis and drying) zone diameter is estimated by [21],

$$D_{pyrolysis} = 3.5 \, D_{th} \tag{23}$$

The height of drying and pyrolysis is calculated from the ratio of the volume of biomass consumed to the cross-sectional area of pyrolysis as follows

$$H_{pyrolysis} = \frac{V_{py}}{A_{py}} = \frac{m_{bm}}{\rho_{bm} \, A_{py}} \qquad (24)$$

The air nozzle area is given as a ratio of 0.05-0.09 from the throat area and it is recommended that the air nozzles will be located around the oxidation zone with a number of 4-6 nozzles in a position to prevent any dark zones in combustion [21]. The diameter at which the air injection starts is in the position where the diameter of the oxidation zone is 2-2.5 of the throat diameter [24]. Air injection at this diameter will keep away the dark zones at oxidation area. The reduction zone diameter is assumed to be the same diameter of the pyrolysis zone.

3. RESULTS AND DISCUSSION

3.1 Optimum height of the reduction zone

Optimum height of the reduction zone is the height at which char in this stage is completely consumed *[10]*. Equation (15) is solved to get the optimum height for the reduction zone and, calculations of the different species concentrations are done and compared based upon this optimum height. That will ensure the consumption of all char in the reduction zone leading to the production of the maximum amount of useful gases with a lower content of CO_2 based on the gasification reactions.

Several factors such as biomass moisture content, air-to-fuel (*AF*) ratio, and temperature at the beginning of reduction affect the height of reduction zone. For example, it was reported in [16] that the height of reduction reduces with an increasing moisture content and air-to-fuel ratio. Figure 3(a) shows the relation between the moisture content and the reduction zone height for Gulmohar, Bamboo, and Neem [25]. It is clearly seen that as the moisture content increases, the height of the reduction zone decreases. This is because higher water content in biomass requires more heat for removal and hence increases the temperature at the oxidation and reduction zones. The temperature increase leads to a direct increase in the reaction rates and hence decreases the height of the reduction zone.

Figure 3(b) illustrates the effect of a varying equivalence ratio on the height of the reduction zone. It also shows that as the equivalence ratio increases, the height decreases. This is

because increasing the equivalence ratio increases the amount of air added and this in turn increases the oxidation temperature and hence the reduction temperature.

The effect of varying the inlet temperature of reduction on the height of reduction zone is presented in Figure 3(c). As the temperature increases, the height decreases because higher temperatures give higher reaction rates as well as formation of different gas species. This affects the destruction of carbon in the reduction zone and hence a decrease in the height as shown.

3.2 Distribution of different gas species along the reduction zone

Gas concentrations and variations along the reduction zone are calculated based on equation (15). Figure 4 shows a linear distribution for all the different gas species in the reduction zone. Rubber wood with MC 20% and Φ 0.32 is used in this case. The reactions in reduction are very fast due to the high temperature in the reduction zone (around 1000 K). The formation of different gas species depends on the velocity, temperature, and concentration of the gas species at the end of combustion zone. Referring to equation (15) which describes the formation of gas species along the reduction zone height, and also Table 6 and Table 7 which describes the reduction reactions and their equivalent rate of formation, higher rates of formation for CO and H_2 are expected. However, variation of CH_4 is very small as its concentration is very small at the beginning of reduction and its formation rate was also small due to lower reaction rates. Formation of CO_2 is expected to decrease along the reduction zone as it is converted into CO based on the reduction reactions. The results also show a good agreement with those reported in [20].

3.3 Gasifier design principles and producer gas composition

Table 8 shows a comparison between the results from the present model and the theoretical design model of [26]. The results show a fairly good agreement for all the dimensions except for the reduction zone length. However, it was stated in [26] that the reduction length was not based on any known calculations but was based on assumptions. While Ref. [10] shows that the reduction zone length varies from 20-50 cm which has a good agreement with the results derived from the present model.

Table 9 shows the ultimate analysis for different feedstocks used in the model. A wide range of biomass materials ($38 \leq C\% \leq 52$, $5.5 \leq H\% \leq 7$, and $36 \leq O\% \leq 45$) are tested with various working conditions to validate the model as presented in

Figure 5. The results of the producer gases also show a fairly good agreement with other experimental results, which further proves the ability of the kinetic model operating under different working conditions for a wide range of biomass composition. Tar formation is also taken into account which was not discussed clearly by any previous numerical models. Additionally, the experimental papers, used for the validation of the producer gases, do not mention the tar formation, thus other experimental data [27] were used to validate the results of the tar formation predicted through the current model. Figure 6- Comparisons between the experimental and present work for the tar yield in producer gas. The results show good agreement which further proves the ability of the present model to simulate tar content in the producer gas.

Figure 7 (a, b) shows the variations of temperature along the gasifier where the maximum temperature is located at the oxidation zone. Higher moisture content levels require more heat for removal in the pyrolysis zone as shown in both the figures. The temperature profile predicted by the kinetic model also has a very good agreement with that of the computational fluid dynamics (CFD) study of biomass gasification carried out recently by Kumar et al. [29] in a downdraft gasifier with a volatile break-up approach.

3.4 Effect of moisture content on the producer gas quality

After validating the current model, it was used to address the optimum working conditions for a gasifier to get higher quality syngas. Figure 8 presents the results of the effect of changing the moisture content on the output producer gas in terms of the higher heating value (HHV) for different feedstocks at a fixed working condition of power (20 kW) and air-to-fuel ratio (0.35). The results clearly show that a lower amount of water content in biomass leads to a significant increase in the heating value which has a good agreement with [11], [8] and [12]. Moreover, lower moisture content leads to a significant increase of CO and H_2 which then leads to an increase of the heating value. In contrast, higher levels of moisture content require more energy for removal, which is never recovered again. This energy loss affects the produced gas and reduces its heating value. The results further show that a decrease of biomass moisture content from 20% to 5% leads to an increase of the produced gas heating value of 10-22%. On the other hand, Figure 9 discusses the effect of moisture content on the produced gas quality. The results show that the higher moisture content leads to an obvious increase of tar content. Tar formation starts from the pyrolysis zone and during combustion, and more water vapour tends to reduce the tar cracking reactions because of a slower reaction rate compared to the CO and H_2 oxidation. The results also show that a decrease of biomass

moisture content from 20% to 5% leads to decrease of tar content of about 18-26%. Based on the current study about the effect of moisture content on the produced gas, lower amount of moisture leads to higher value gases with a lower amount of tar. Recommended values of moisture content those give a higher yield and quality of syngas must be no more than 10%.

3.5 Effect of equivalence ratio on the producer gas quality

Figure 10 illustrates the effect of changing the equivalence ratio on the producer gas heating value for different feedstocks at fixed working conditions of power (20 kW), and moisture content (10%). The results show a gradual increase of the heating value with a decreasing equivalence ratio. Referring to the oxidation reactions and their equivalent rate (Table 4), more air supply in the combustion zone encourages the oxidation reactions to occur with more CO_2 and H_2O. This also leads to a decrease in the tar content due to the tar cracking reaction that takes place with more oxygen supply in the oxidation zone, as clearly seen in Figure 11. Moreover, the results show an increase in the producer gas heating value of 25-30% while decreasing Φ from 0.4 to 0.2. Tar yield also increases from 16% to 50% with the same level of magnitude drop in Φ. Complex tar compounds were not taken into account in the current study, and the tar cracking in model depends only on the combustion reactions in Table 4 and Table 5.

In conclusion an equivalence ratio of 0.3-0.35 with lower amounts of moisture content less than 10%, gives a higher yield of syngas composition with reasonable amounts of tar content. In particular, woody biomass materials give a higher yield of syngas while olive wood has a heating value up to 6.4 MJ/Nm^3 at Φ=0.2 and MC of 10%. Higher value of Φ gives a lower heating value for wood pellets and saw dust. The tar content was also lower for wood (1.65%) at Φ=0.4.

3.6 Gasifier design and operating conditions

Table 10 illustrates the effect of changing the biomass type on the gasifier design. The results show a variation in the fuel feeding rate dependant on the biomass composition from C, H, and O. There are also small variations predicted in the oxidation and reduction height, pyrolysis and throat diameter, and air injection area. The gasifier dimensions are quite similar for all the types except for the rice husk. Rice husk has very low carbon and hydrogen content which affect the heating value of biomass. The decrease in the heating value (based on

equation (21)) leads to an increase in biomass feeding rate, and hence an increase in the corresponding gasifier dimensions to accommodate the higher mass and volume of biomass. Varying the thermal power is found to affect the gasifier dimensions, but it has no effect on the gas composition. The effect of changing thermal power is related to the fuel feeding rate which is again related to the volume occupied by biomass inside the gasifier and thus, it changes the gasifier design. While changing both of the moisture content or equivalence ratio (Φ) analysed in the previous sections have a great effect on the gas composition and its heating value, it is found to have no effect on the gasifier design.

3.7 Key design parameters and its effect on the working conditions

Throat diameter and fuel feeding rate are the key parameters in designing a gasifier. All the other dimensions can be generated using these two parameters. As a result, studying the effect of varying thermal power from 1kW to 1MW for different biomass types is shown in Figure 12 and Figure 13. Figure 12 shows the effect of changing required thermal power on the throat diameter design. The results show higher throat area for higher power. This is because higher power requires more biomass feeding and hence, bigger volume for pyrolysis and combustion zones.

Figure 13 shows the effect of changing the required thermal power on the biomass feeding rate. The results show a linear variation for the feeding rate as it is calculated from equation (21) which is a linear relation between the thermal power, feeding rate, and biomass heating value.

4. CONCLUSION

The current work presents a four-zone kinetic model for a downdraft gasifier in which the gasification products are determined using a novel approach that includes an optimum length of the reduction zone. It gives accurate results for the producer gas composition, tar content, and gives also predictions for the dimensions of a downdraft gasifier. Previous models never combined the gas composition, tar content, and gasifier dimensions in one work.

The design theory in this model was built based on the optimum height of the reduction zone, which was not discussed before in any published work. Finally, the results from this model was used to test a wide range of biomass materials to conclude the optimum working conditions and best feedstocks that give higher yields of syngas with a lower tar content. Key

design parameters for a downdraft gasifier are mentioned and the effects on the working conditions are discussed using the current model.

An equivalence ratio of 0.3-0.35 with lower amounts of moisture content less than 10%, gives a higher yield of syngas composition with reasonable amounts of tar content. In particular, woody biomass materials give a higher yield of syngas while olive wood has a heating value up to 6.4 MJ/Nm^3 at Φ=0.2 and MC of 10%. The tar content was also lower for wood (1.65%) at Φ=0.4.

Future work on the model will try to incorporate a tar destruction system with new techniques to further increase the producer gas heating value.

ACKNOWLEDGMENTS

REFERENCES

[1] Basu P., Biomass Gasification, Pyrolysis, and Torrefaction. Practical Design and Theory. Second Edition, Amsterdam: Academic Press, 2013.

[2] Sepe AM, Li J, and Paul MC, "Assessing biomass steam gasification technologies using a multi-purpose model," *Energy Conversion and Management,* vol. 129, pp. 216-226, 2016.

[3] Yan L, Cao Y, and He B, "On the kinetic modeling of biomass/coal char co-gasification with steam," *Chemical Engineering Journal,* vol. 331, pp. 435-442, 2018.

[4] Li J, Paul MC, Younger PL, Watson I, Hossain M, and Welch S, "Prediction of high-temperature rapid combustion behaviour of woody biomass particles," *Fuel,* vol. 165, pp. 205-214, 2016.

[5] Li XT, Grace JR, Lim CJ, Watkinson AP, Chen HP, Kim JR, "Biomass gasification in a circulating fluidized bed.," *Biomass and Bioenergy,* p. 171–193, 2004.

[6] Salem AM, Kumar U, A. Izaharuddin AN, Dhami H, Sutardi T, and Paul MC, "Advanced numerical methods for the assessment of integrated gasification and CHP generation technologies," in *De S., Agarwal A., Moholkar V., Thallada B. (eds) Coal and Biomass Gasification. Energy, Environment, and Sustainability*, Springer, 2018, pp. 307-330.

[7]   Altafini CR, Wander PR, Barreto RM, "Prediction of the working parameters of a wood waste gasifier through an equilibrium model," *Energy Conversion and Management,* vol. 44, p. 2763–77, 2003.

[8]   Budhathoki R., Three zone modeling of Downdraft biomass Gasification: Equilibrium and finite Kinetic Approach" MSC Thesis,, University of Jyväskylä, 2003.

[9]   Channiwala SA, Ratnadhariya JK., "Three zone equilibrium and kinetic free modeling of biomass gasifier – a novel approach," *Renewable Energy,* vol. 34, no. 4, p. 1050–1058, April 2009.

[10]   Dejtrakulwong C, Patumsawa S., "Four Zones Modeling of the Downdraft Biomass Gasification Process: Effects of moisture content and air to fuel ratio," *Energy Procedia,* vol. 52, p. 142 – 149, 2014.

[11]   Zainal ZA, Ali R, Lean CH, Seetharamu KN., "Prediction of performance of a downdraft gasifier using equilibrium modeling for different biomass materials," *Energy Conversion and Management,* vol. 42, no. 12, p. 1499–1515, August 2001.

[12]   Dutta A, Jarungthammachote S., "Thermodynamic equilibrium model and second law analysis of a downdraft waste gasifier," *Energy,* vol. 32, pp. 1660-1669, 2007.

[13]   Koroneos C, Lykidou S., "Equilibrium modeling for a downdraft biomass gasifier for cotton stalks biomass in comparison with experimental data," *Journal of Chemical Engineering and Materials Science,* vol. 2, no. 4, pp. 61-68, April 2011.

[14]   Vaezi M, Fard MP, Moghiman M., "On a Numerical Model for Gasification of Biomass Materials," in *1st WSEAS Int. Conf. on COMPUTATIONAL CHEMISTRY*, Cairo, Egypt, December 29-31, 2007.

[15]   Giltrap DL, McKibbin R, Barnes GRG, "A steady state model of gas-char reactions in a downdraft biomass gasifier," *Solar Energy 74,* p. 85–91, 2003.

[16]   Sharma AK., "Modeling and simulation of a downdraft biomass gasifier 1. Model development and validation," *Energy Conversion and Management 52,* p. 1386–1396, 2011.

[17]   Roy PC, Chakraborty N., "Modelling of a downdraft biomass gasifier with finite rate kinetics in the reduction zone," *International Journal of Energy Research,* pp. 833-51, 2009.

[18]   Babu BV, Chaurasia AS, "Modeling, simulation and estimation of optimum parameters in pyrolysis of biomass," *Energy Conversion and Management 44,* p. 2135–2158, 2003.

[19]   Bridgewater R, Shand A., "Fuel gas from biomass: Status and new modeling approaches," *Thermochemical Processing of Biomass,* pp. 229-254, 1984,.

[20]   Sheth PN. Babu BV., "Modeling and simulation of reduction zone of downdraft biomass gasifier: Effect of char reactivity factor," *Energy Conversion and Management,* vol. 47, pp. 2602-2611,

9,2006.

[21] Rathore NS, Panwar NL, Chiplunkar YV., "Design and techno economic evaluation of biomass gasifier for industrial thermal applications," *African Journal of Environmental Science and Technology.,* vol. 3, no. 1, pp. 6-12, 2009.

[22] Reed TB, Das A., Handbook of Biomass Downdraft Gasifier Engine Systems., Solar Energy Research Institute, USA, 1988.

[23] Sivakumar S, Ranjithkumar N, Ragunathan S., "Design and Development of Down Draft Wood Gasifier," *International Journal of Mechanical Engineering,* vol. 2, no. 2, pp. 1-10, May 2013.

[24] Sivakumar S, Pitchandi K, Natarajan E., "Modelling and simulation of down draft wood gasifier," *Journal of Applied Sciences.,* vol. 8, no. 1, pp. 271-279, 2008.

[25] Dutta PP, Pandey V, Das AR, Sen S, Baruah DC, "Down Draft Gasification Modelling and Experimentation of Some Indigenous Biomass for Thermal Applications," *Energy Procedia 54,* p. 21 – 34, 2014.

[26] Orisaleye JI, Ojolo SJ., "Design and Development of a Laboratory Scale Biomass Gasifier," *Journal of Energy and Power Engineering,* vol. 4, no. 8, pp. 16-23, Aug, 2010.

[27] Jayah TH, Aye L, Fuller RJ, Stewart DF, "Computer simulation of a downdraft wood gasifier for tea drying," *Biomass and Bioenergy,* vol. 25, pp. 459-469, 2003.

[28] Qin Y, Campen A, Wiltowski T, Feng J, Li W., "The influence of different chemical compositions in biomass on gasification tar formation," *Biomass and Bioenergy,* vol. 83, pp. 77-84, 2015.

[29] Kumar U, Salem AM and Paul MC, "Investigating the thermochemical conversion of biomass in a downdraft gasifier with a volatile break-up approach," *Energy Procedia,* pp. EGYPRO33517, PII S1876610217358605, 2017.

[30] Koufopanosi CA, Maschio G, Lucchesit A., "Kinetic Modelling of the Pyrolysis of Biomass and Biomass Components," *The Canadian Journal of Chemical Engineering,* vol. 67, FEB, 1989.

[31] Tinaut FV, Melgar A, Pérez JF, Horrillo A., "Effect of biomass particle size and air superficial velocity on the gasification process in a downdraft fixed bed gasifier. An experimental and modelling study," *Fuel Processing Technology,* vol. 89, p. 1076– 1089, 2008.

[32] Fossum M, Barrio M., "Operational characteristics of a small-scale stratified downdraft gasifier," in *Technologies and Combustion for a Clean Environment Sixth International Conference*, 2001.

[33] Zainal ZA, Ali R, Lean CH, Seetharamu KN, "Prediction of performance of a downdraft gasifier using equilibrium modeling for different biomass materials," *Energy Conversion and Management, vol. 42,* pp. 1499-1515, 2001.

[34] Aiello RC, Pedroso DT, "Biomass gasification on a new really tar free downdraft gasifier," *Rev. ciênc. exatas, Taubaté,* pp. 59-62, 2005.

[35] Yoon SJ, Son YI, Kim YK, Lee J., "Gasification and power generation characteristics of rice husk and rice husk pellet using a downdraft fixed-bed gasifier," *Renewable Energy 42,* pp. 163-167, 2012.

[36] Barrio M, Fossum M, "Operational characteristics of a small-scale stratified downdraft gasifier," in *Technologies and Combustion for a Clean Environment Sixth International Conference*, 2001.

[37] Yoon SJ, Son Y, Kim Y, Lee J., "Gasification and power generation characteristics of rice husk and rice husk pellet using a downdraft fixed-bed gasifier," *Renewable Energy,* vol. 42, p. 163–167, 2012.

NOMENCLATURE

Upper case letters   **Abbreviations**

A	Pre-exponential factor, (s^{-1})	B	biomass
C	Concentration (mol/m^3)	C	char
D	Diameter (m)		
E	Energy, (kJ/mol)	MC	Moisture content, (%)
H	Enthalpy, (kJ/mol	A/F	Air to fuel ratio

K	Kinetic constant, (s^{-1})	ER	Equivalence ratio
M	Molecular mass, (kg/mol)	CRF	Char reactivity factor
P	Pressure, (Pa)	HR	Heating rate, $(K\ s^{-1})$
GH	Hearth Load $(Nm^3/\ (h.m^2))$	HHV	Higher heating value (kJ/kg)
T	Temperature, (K)	G	gases
R	Net rate of formation, $(mol\ m^{-3}s^{-1})$	Nm^3	Normal cubic meter
V	Volume (m^3)	py	pyrolysis
W	Power (W)	**Subscripts**	
		A	
			atmospheric

Lower case letters

		d	drying
c_p	Specific heat at const. pressure, $(J.\ mol^{-1}\ .\ K^{-1})$	f	fuel
m	Mass, (kg)	g	Gases
n	no. of moles, (mol)	i	Species
r	Reaction rate, $(mol\ m^{-3}s^{-1})$	l	liquid
t	Time, (s)	th	thermal
v	Velocity, (ms^{-1})		
y	composition fraction	**Greek letters**	
z	Height, (m)	ρ	Density
		$\sum$	Summation
		Δ	Change in state

List of figures and tables

Table 1- Data for the drying model *[10]*

A_d (s^{-1})	K_d, (s^{-1})	E_d, (kJ mol^{-1})	T_d, (K)
5.13×10^6	0.1652	88	400

Table 2- Parameters of the pyrolysis model [30] and [18].

R	A (s^{-1})	D (K)	L (K^2)	E (kJ mol^{-1})
1	9.973 ×10^{-5}	17254.4	-9061227	
2	1.068×10^{-3}	10224.4	-6123081	81
3	5.7×10^5			

Table 3- Optimum values of non-isothermal pyrolysis [18].

T (K)	HR (Ks^{-1})	Time (s)	n_1	$n_2 = n_3$
1259	51	9.53	1	1.5

Table 4- Oxidation reactions ([16] and [31]).

R	Reaction	A_j	E_j/R
1	$H_2 + 0.5\ O_2 \leftrightarrow H_2O$	1.6×10^9	3420
2	$CO + 0.5\ O_2 \leftrightarrow CO_2$	1.3×10^8	15106
3	$CH_4 + 1.5\ O_2 \leftrightarrow CO + 2H_2O$	1.585×10^9	24157
4	$C_6H_{6.62}O_{0.2} + 4.45\ O_2 \leftrightarrow 6CO + 3.1H_2O$	2.07×10^4	41646
5	$C + 0.5\ O_2 \leftrightarrow CO$	0.554	10824

Table 5- Rate expressions for oxidation reactions ([16] and [31]).

R	Reaction rate (mol m^{-3} s^{-1})
1	$r_{H_2} = A_1 T^{1.5} exp\left(-\dfrac{E_{co}}{RT}\right).[C_{co_2}][C_{H_2}]^{1.5}$
2	$r_{co} = A_2\ exp\left(-\dfrac{E_{co}}{RT}\right).[C_{co}][C_{o_2}]^{0.25}[C_{H_2O}]^{0.5}$
3	$r_{CH_4} = A_3\ exp\left(-\dfrac{E_{CH_4}}{RT}\right).[C_{o_2}]^{0.8}[C_{CH_4}]^{0.7}$
4	$r_{tar} = A_4\ T.P_A^{0.3}.exp\left(-\dfrac{E_{tar}}{RT}\right).[C_{o_2}][C_{tar}]^{0.5}$

5	$$r_C = A_5 \, exp\left(-\frac{E_{char}}{RT}\right).[C_{o_2}]$$

Table 6- Reduction reactions *[15]* .

R	Reactions		A (1/s)	E (kJ mol^{-1})
1	Boudouard	$C + CO_2 \leftrightarrow 2\,CO$	36.16	77.39
2	Water-gas	$C + H_2O \leftrightarrow CO + H_2$	1.517×10^4	121.62
3	Methane formation	$C + 2H_2 \leftrightarrow CH_4$	4.189×10^{-3}	19.21
4	Steam Reforming	$CH_4 + H_2O \leftrightarrow CO + 3H_2$	7.301×10^{-2}	36.15

Table 7- Rate expressions for the reduction reactions [15] .

R	Reaction rates (mol m^{-3} s^{-1})
1	$$r_1 = A_1 \, exp\left(-\frac{E_1}{RT}\right).\left(y_{CO_2} - \frac{y^2_{CO}}{K_{eq,1}}\right)$$
2	$$r_2 = A_2 \, exp\left(-\frac{E_2}{RT}\right).\left(y_{H_2O} - \frac{y_{CO}\cdot y_{H_2}}{K_{eq,2}}.\right)$$
3	$$r_3 = A_3 \, exp\left(-\frac{E_3}{RT}\right).\left(y^2_{H_2} - \frac{y_{CH_4}}{K_{eq,3}}\right)$$
4	$$r_4 = A_4 \, exp\left(-\frac{E_4}{RT}\right).\left(y_{CH_4}y_{H_2O} - \frac{y_{CO}\cdot y^3_{H_2}}{K_{eq,4}}\right)$$

Table 8- Comparison between the present and theoretical work for gasifier dimensions

Working parameters	20 kW power, Palm shell , MC 14%, $\Phi = 0.3$	
	Model	Ojolo, [26]
Fuel feed (kg hr^{-1})	4.0	4.32
H_{pyr} (cm)	48.9	40
H_{oxd} (cm)	11	---
H_{red} (cm)	30.9	15 $20 - 50$ [6]
D_{pyr} (cm)	22.4	23.8
D_{throat} (cm)	6.4	6.8
$D_{air\ injection}$ (cm)	17.9	20

Table 9- Ultimate analysis for different feedstocks used in model.

	Biomass type	C %	H %	O %	Experiment results from
1	Rubber wood	50.6	6.5	42	[27]
2	Wood Pellets	50.7	6.9	42.4	[32]
3	Gulmohar	44.43	6.16	41.9	[25]
4	Bamboo	48.39	5.86	39.21	[25]
5	Neem	45.1	6	41.5	[25]
6	Dimaru	44.85	5.98	41.84	[25]
7	Sisham	45.85	5.8	40.25	[25]
8	Saw Dust	52	6.07	41.55	[7]
9	Wood	50	6	44	[33]
10	Olive wood	46.43	5.63	44.91	[34]
11	Rice husk	38.5	5.5	36.6	[35]

Table 10- Effect of changing biomass on the gasifier design.

Biomass	Rubber wood	Wood Pellets	Gulmohar	Wood	Saw Dust	Rice husk
Fuel feed (kg hr^{-1})	3.65	3.52	4.51	3.8	3.65	6.3
H_{pyr} (cm)	48.8	48.9	49.1	48.7	48.9	48.9
H_{oxd} (cm)	10.9	10.7	12.1	11.2	10.9	14.4
H_{red} (cm)	33.02	29.9	31.3	31.2	29.1	30.2
D_{pyr} (cm)	21.8	21.4	24.2	22.34	21.8	28.7
D_{throat} (cm)	6.23	6.11	6.9	6.4	6.23	8.1
$D_{air\ injection}$ (cm)	17.4	17.1	19.4	17.8	17.4	22.9
Total air area (cm^2)	2.13	2.1	2.6	2.24	2.13	3.6
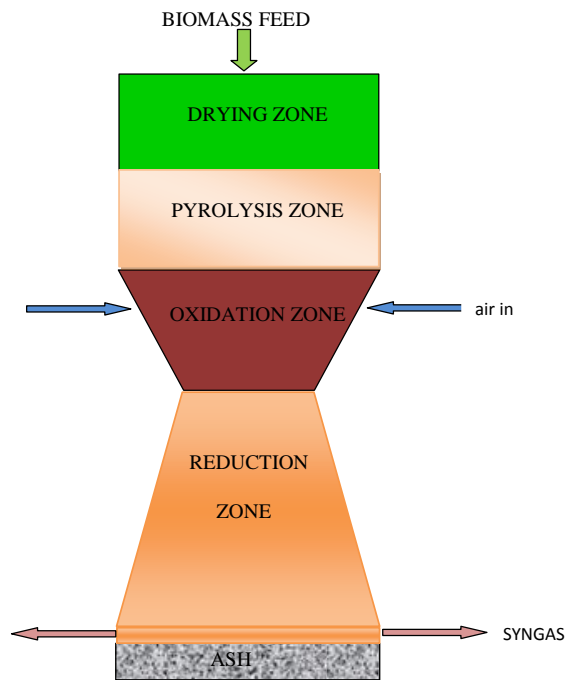
Figure 1- Schematic view of a downdraft gasifier.
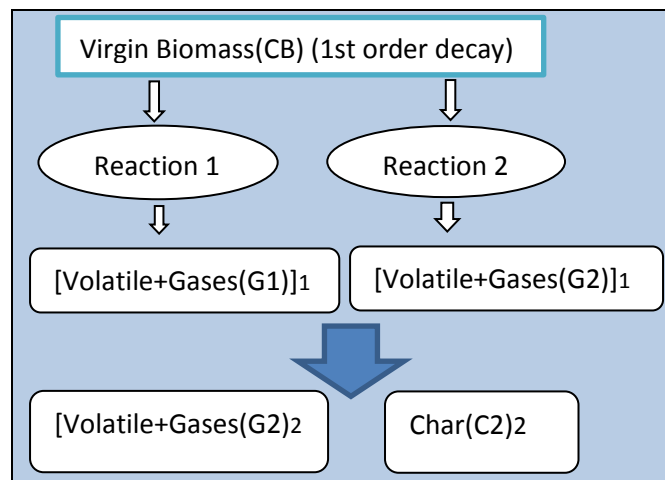
Figure 2- Biomass devolatization.
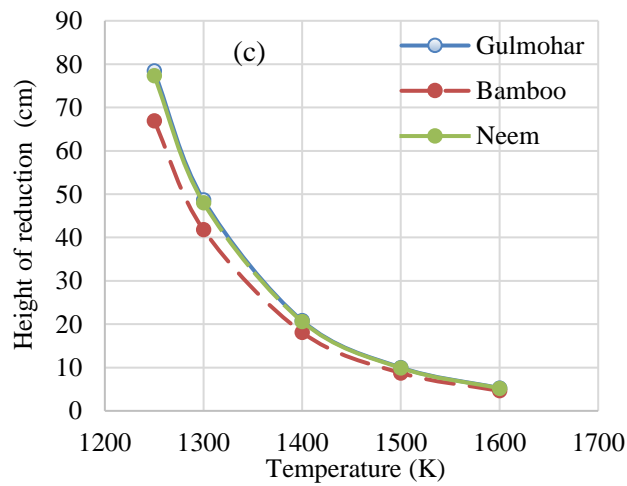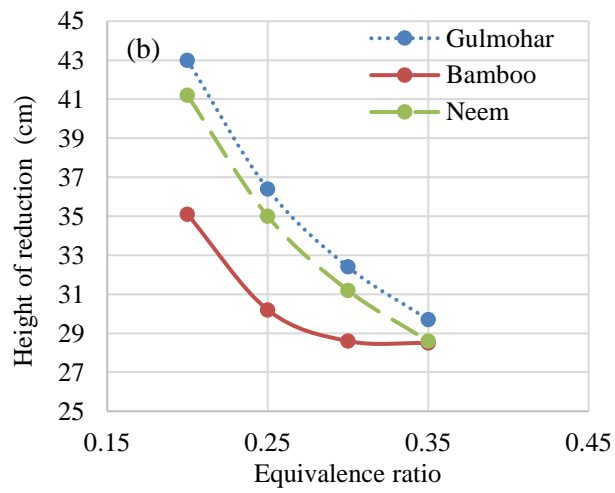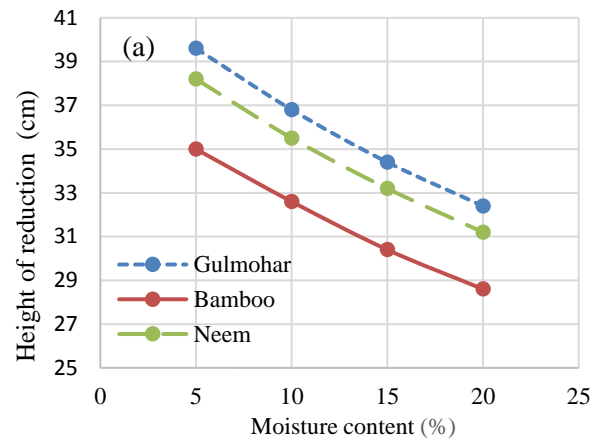
Figure 3- Effect of varying moisture content (a), equivalence ratio (b) and temperature (c) on the height of reduction zone.
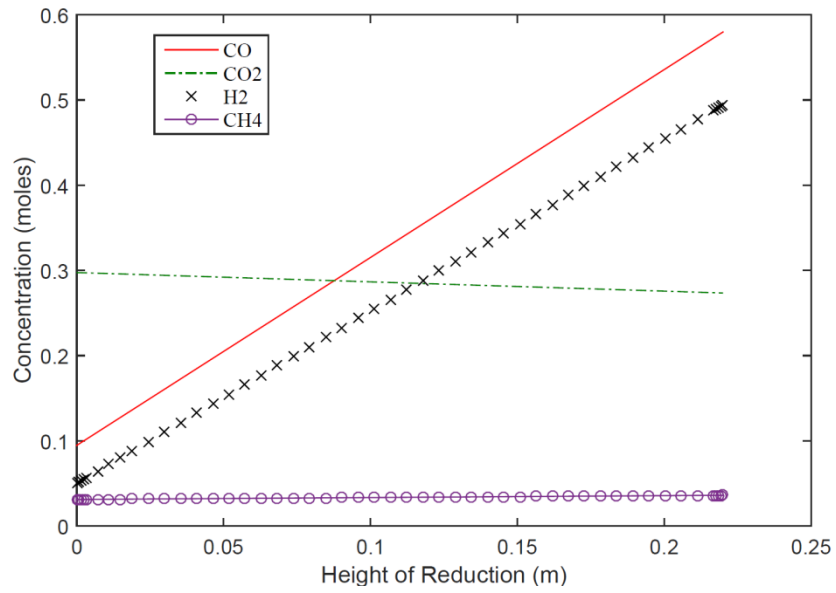
Figure 4- Variation of different gas species concentrations for Rubber wood along the reduction zone
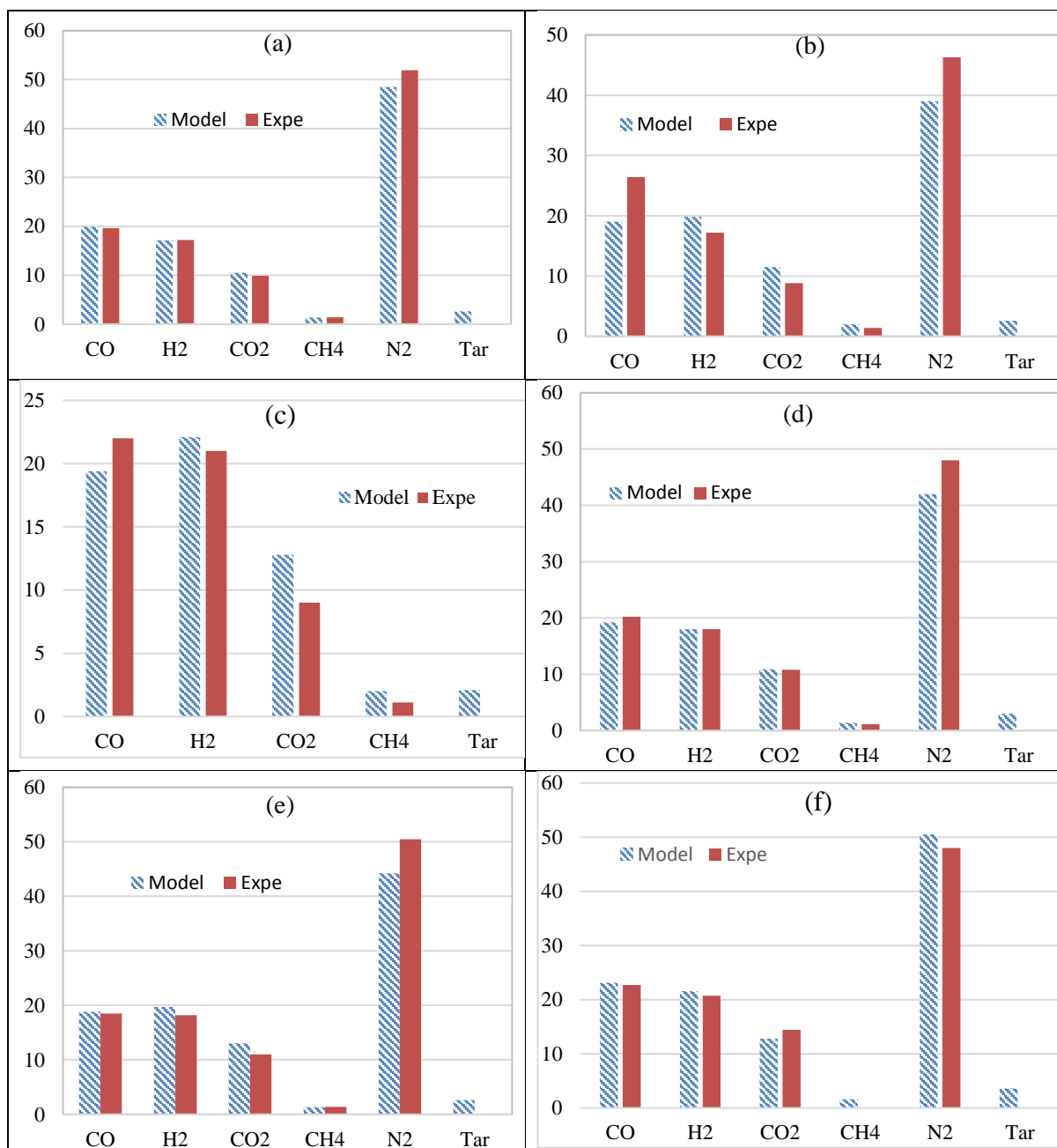
Figure 5- Comparison for gas volumetric composition (vertical axis) between the present work and other experimental work for same (feedstock, *Φ*, and MC), (a) Rubber wood [27], (b) Wood pellets [36], (c) rice husk [37], (d) Bamboo [25], (e) Neem [25], and (f)
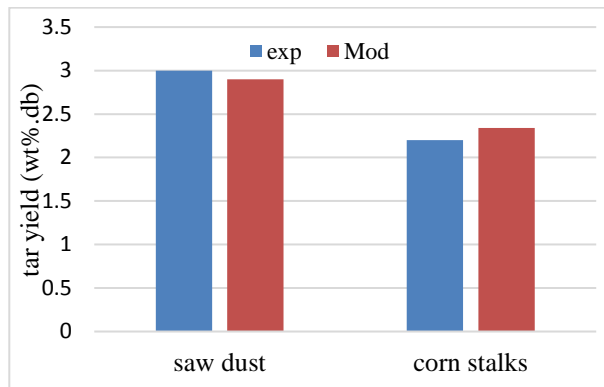
Figure 6- Comparisons between the experimental *[28]* and present work for the tar yield in producer gas.
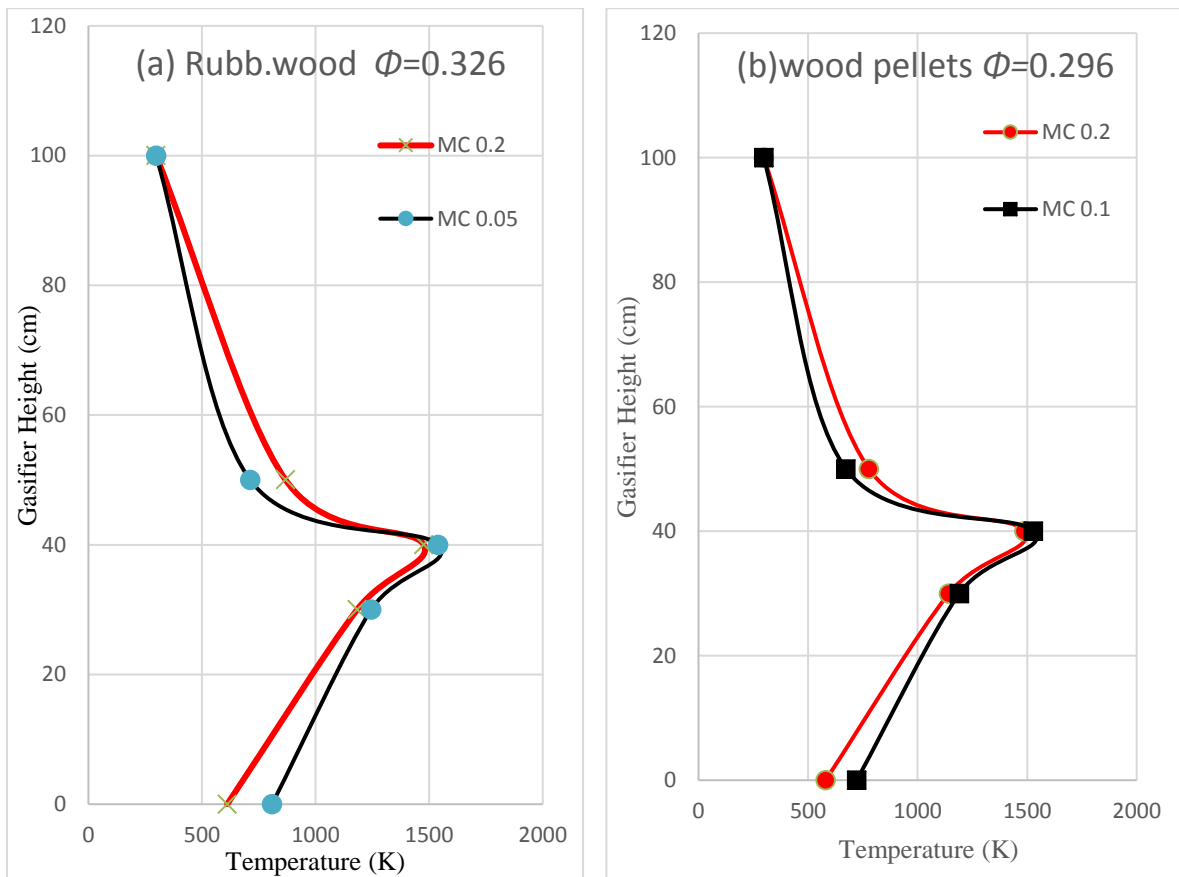
Figure 7(a) Temperature profile along the gasifier for rubber wood   (b)- Temperature profile along the gasifier for wood pellets
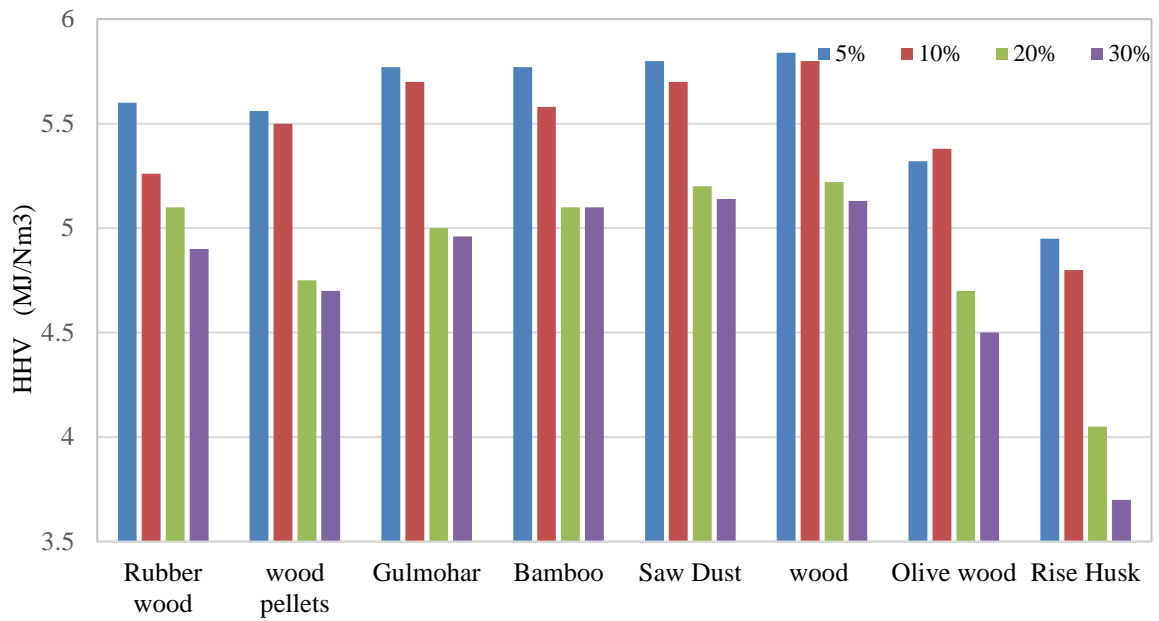
Figure 8- Effect of changing moisture content on producer gas heating value.
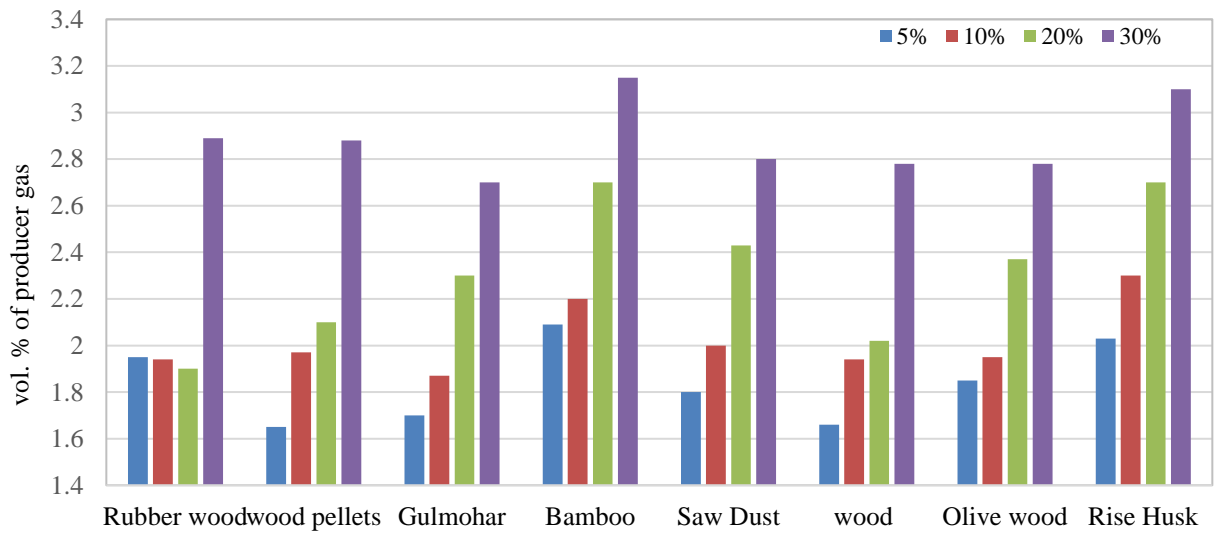
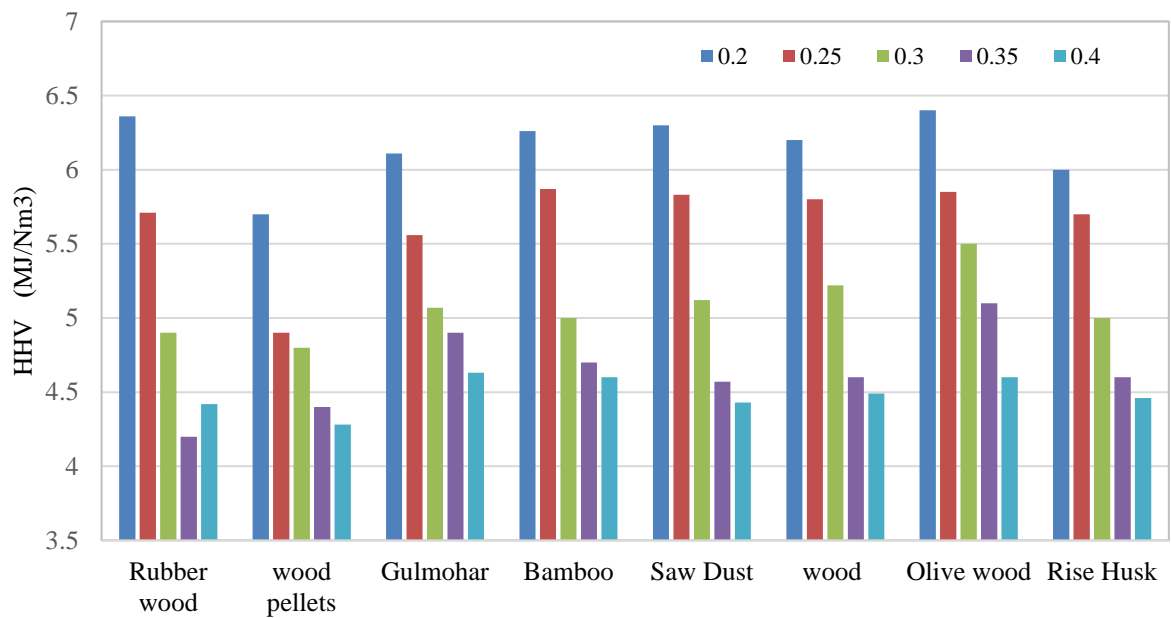Figure 9- Effect of changing moisture content on producer gas tar content.

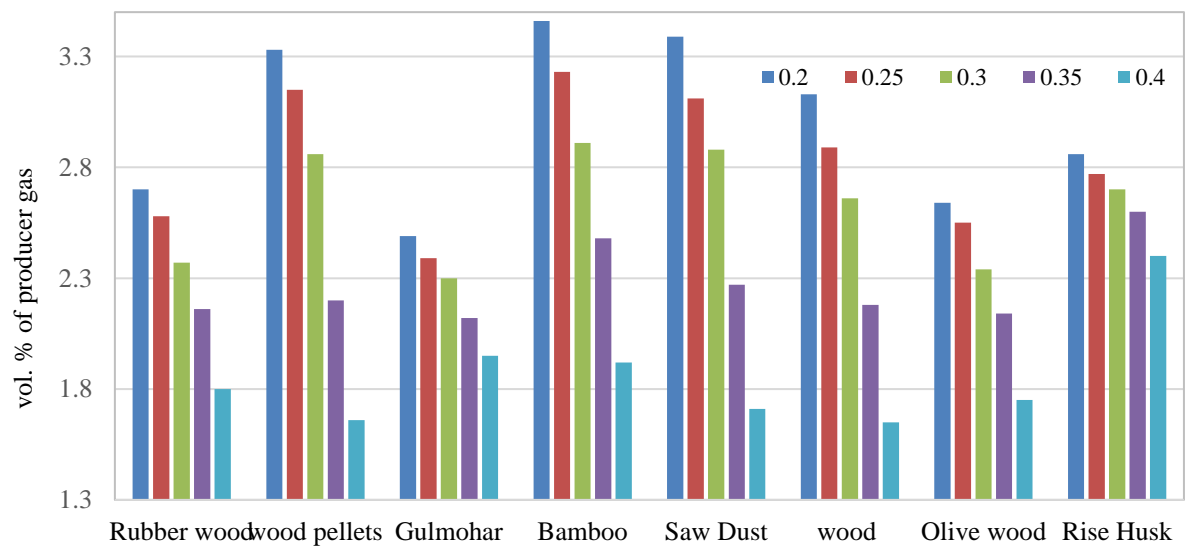Figure 10- Effect of changing equivalence ratio on producer gas heating value.

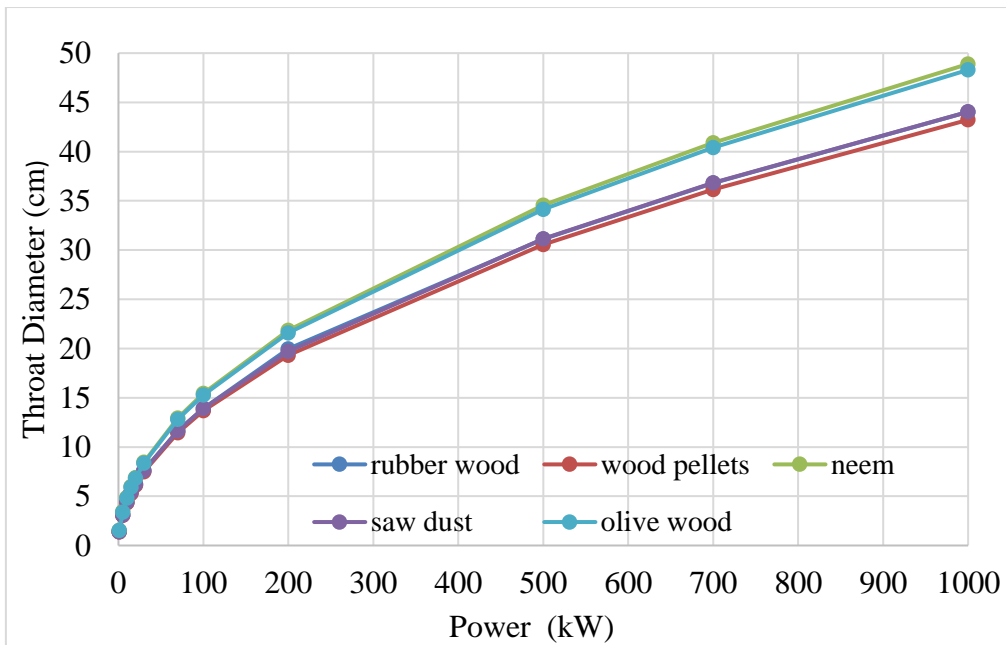Figure 11- Effect of changing equivalence ratio on producer gas tar content.

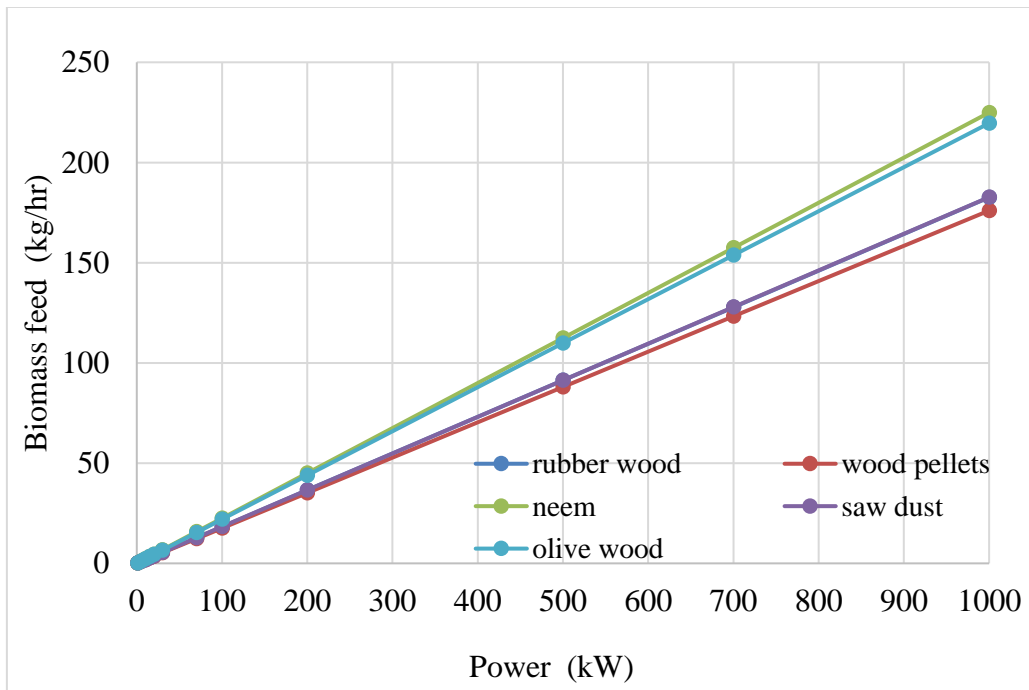Figure 12- Effect of changing power on gasifier throat diameter.

Figure 13- Effect of changing power on biomass feeding rate.